

# Backcasting the Optimal Decisions in Transport Systems: An Example with Electric Vehicle Purchase Incentives

Dr. Vinith Lakshmanan\*, Xavier Guichet, and Antonio Sciarretta

IFP Energies nouvelles, France

## SHORT SUMMARY

This study represents a first attempt to build a backcasting methodology to identify the optimal policy roadmaps in transport systems. In this methodology, desired objectives are set by decision makers at a given time horizon, and then the optimal combinations of policies to achieve these objectives are computed as a function of time (i.e., “backcasted”). This approach is illustrated on the transportation sector by considering a specific subsystem with a single policy decision. The subsystem describes the evolution of the passenger car fleet within a given region and its impact on greenhouse gas emissions. The optimized policy is a monetary incentive for the purchase of electric vehicles while minimizing the total budget of the state and achieving a desired CO<sub>2</sub> target. A case study applied to Metropolitan France is presented to illustrate the approach. Additionally, alternative policy scenarios are also analyzed to provide further insights.

**Keywords:** Backcasting, Transport systems, Policy making, Environmental Impacts

## 1 INTRODUCTION

The European Union’s (EU) goal of carbon neutrality by 2050 requires a 90% reduction in emissions from the transport sector compared to 1990 levels. The European Commission has therefore adopted a package of proposals to put EU policies on track to reduce net greenhouse gas emissions by at least 55% by 2030 (European Commission (2021)).

Governance, policies and incentives (“decisions”) play an important role in shaping the transport systems of the future, influencing the development and implementation of different technologies and modes of transport. It is therefore important to examine how decisions can best be used to steer them in the desired direction of decarbonisation.

The traditional approach to finding policy roadmaps involves designing prospective scenarios, simulating their impacts, and drawing conclusions about effective decisions. However, this method limits choices to predefined scenarios, which represent only a small subset of possibilities. As a result, the optimum may not be reached since only selected scenarios are evaluated.

To overcome these limitations, a novel (“backcasting”) paradigm is supported in this work. In this approach, desired objectives are set by decision makers at a given time horizon, and the optimal combinations of policies to achieve these objectives are computed as a function of time (“backcasted”). In this way, the a priori choice of scenarios is replaced by a fully dynamic optimisation process that can explore all possible combinations.

The backcasting paradigm has been introduced since the last century (Robinson (1982); Bibri & Krogstie (2019)). It has mainly been used in a qualitative way (Papazikou et al. (2020)) or in a quantitative way with a static optimisation procedure (Gomi et al. (2011); Ashina et al. (2012)). However, this process can be more effectively cast as an optimal control problem, with a suitable definition of an objective function, a horizon, local and terminal constraints, etc.

Of course, since future impacts must be predicted, the new backcasting paradigm is still based on a simulation model.

This model must be able to describe transport as a system, with controllable inputs, exogenous inputs, outputs, and states. The manipulable inputs represent the decisions to be optimized, which may concern local and state authorities, the EU, or even private companies. The exogenous inputs represent the influence of other related systems, such as energy, urban, economic, demographic. The outputs represent the desired effects or the constraints to be imposed on the backcasting process. Finally, the states are the dynamics associated with the internal variables.

In this paper, we illustrate the backcasting paradigm applied to the transport sector by considering a specific subsystem with a single decision variable. The considered subsystem describes the

evolution of the passenger car fleet within a given region and its impact on greenhouse gas emissions. The optimized decision is a monetary incentive for the purchase of electric vehicles.

The prediction of fleet composition is the subject of a large body of literature (De Ceuster et al. (2004); Van Grol et al. (2016); ITF (2019); Bouter et al. (2022)). Typically, dynamic fleet models are based on the evaluation of stocks and sales of different types of vehicles per time period. Stocks change over time due to the disposal of old vehicles (due to scrapping, export, change of use, etc.) and sales of new vehicles. The latter, in turn, are induced by transport demand (vkm) and mileage, and are split among vehicle types using discrete choice models (Train (2003); Ben-Akiva & Lerman (2000)).

The GHG emissions of a given vehicle fleet are typically assessed using emission factors. CO<sub>2</sub> emissions of light-duty vehicles are regulated in the EU. Similar regulations are about to be applied to heavy-duty vehicles.

Recent studies that include electric vehicles have applied a fleet model to predict the future transportation emissions in France (Bouter et al. (2022); ITF (2019)), Norway (Thorne et al. (2021)), Japan (Kenta & Nakata (2020)), and the U.S. (Woody et al. (2023)).

The paper is organized as follows. Section 2 outlines the backcasting methodology, including system model assumptions, a reduced-order model of passenger car fleet evolution, and the backcasting problem formulation with its semi-analytical solution. A full-order model and its OCP formulation are then presented. Section 3 discusses case study applied to France targeting 2050 CO<sub>2</sub> emissions using the full-order model. Finally, Sect. 4 provides conclusions and suggests directions for making it more realistic.

## 2 METHODOLOGY

### *Assumptions*

In this study, the backcasting process optimizes the government's monetary incentive  $u(t)$  (€) for the purchase of electric vehicles (EV) to meet a target for greenhouse gas emissions (CO<sub>2</sub>) in year  $T$ . The system is represented by an aggregate dynamic model that computes CO<sub>2</sub> emissions over time  $t$  with a one-year time step.

We consider only a single zone of interest and only private vehicles as the mode of transportation. The latter is composed of two vehicle types (thermal,  $v = 1$  and electric,  $v = 2$ ). Additionally, the vehicles are distinguished by  $A+1$  age classes ( $a = 0 \dots A$ ), where  $a = 0$  corresponds to new vehicles sold. The vehicle stock by type and age in year  $t$  is denoted as  $S_{va}(t)$ , and its survival rate over time due to factors such as scrappage, wear, and obsolescence, is modeled using an age-dependent factor  $\eta_a$ .

Several model inputs are considered exogenous such as transport demand  $G(t)$  (vehicle-km), mileage  $M(t)$  (km/y), and purchase and operating costs (i.e., fuel, maintenance, and insurance) by vehicle type (€). The latter are considered as the main determinants for the choice of new vehicles, alongside the development rate of refueling infrastructure. Conversely, socio-economic factors like age, gender, and income are not explicitly considered; instead, an adoption coefficient based on the Bass model (Bass (1969)) is used to model new technology adoption, such as the EV (McManus & Senter (2009); Struben & Sterman (2008)).

Tailpipe CO<sub>2</sub> emissions  $E(t)$  are described using emission factors  $\epsilon_{1a}$  (g/km) for thermal vehicles distinguished by age. Obviously,  $\epsilon_{2a} \equiv 0$ . Additionally, cumulative emissions  $\mathcal{E}(t)$  represent the sum of the yearly CO<sub>2</sub> emissions from the present until year  $t$ .

### *Modeling and backcasting: Reduced-order model*

We first derive a simple model with constant mileage  $M$ , two age classes, i.e., new and old vehicles ( $A = 1$ ), and a constant survival rate  $\eta$ . Therefore, we remove the age index and denote the stock of new vehicle by  $N(t)$  and that of old vehicles by  $O(t)$ . Under these assumptions, the total stock always equals the transport demand, i.e.,  $S(t) = N(t) + O(t) = S_1(t) + S_2(t) \equiv G(t)/M$ .

The model can be summarized as follows

$$E(t) = \epsilon_1 M S_1(t) , \tag{1}$$

$$S_1(t) = \eta S_1(t-1) + N(t) P_1(t, u(t)) , \tag{2}$$

$$\mathcal{E}(t) = \mathcal{E}(t-1) + \epsilon_1 M S_1(t) , \tag{3}$$

$$P_1(t, u(t)) = \frac{\mathcal{P}(t)}{\mathcal{P}(t) + \mathcal{Q}(t)\mathcal{R}(t)u(t)}, \quad (4)$$

where

$$N(t) = \frac{G(t) - \eta G(t-1)}{M} \quad (5)$$

$$\mathcal{P}(t) = e^{\mu U_1(t)} \quad (6)$$

$$\mathcal{Q}(t) = \exp \left( \mu(1 - c_2^A(t)) \left( p^P \frac{C_2^P(t)}{\overline{C}^P(t)} + p^O \frac{C_2^O(t)}{\overline{C}^O(t)} + p^I(1 - c_2^I(t)) \right) \right), \quad (7)$$

and

$$\mathcal{R}(t) = \exp \left( -\mu(1 - c_2^A(t)) \frac{p^P}{\overline{C}^P(t)} \right) \quad (8)$$

are explicit functions of time only.

The latter derive from a logit discrete choice model based on a utility function defined as

$$U_v(t) = (1 - c_v^A(t)) \left( p^P \frac{C_v^P(t) - u_v(t)}{\overline{C}^P(t)} + p^O \frac{C_v^O(t)}{\overline{C}^O(t)} + p^I(1 - c_v^I(t)) \right), \quad (9)$$

i.e., the product of an adoption-based factor and a cost-based factor. In the latter,  $C_v^P$  is the purchase price,  $C_v^O$  is the sum of operating costs,  $c_v^I$  is the rate of development of the refueling infrastructure (normalized to unity, by definition  $c_1^I \equiv 1$ ), and  $p$  are tuning coefficients. The average costs between the two vehicle types are given by  $\overline{C}^P(t)$  and  $\overline{C}^O(t)$ . In the adoption-based utility factor,  $\mu$  is a tuning coefficient and  $c_2^A$  ( $c_1^A \equiv 0$ ) is the adoption coefficient. Since the cost-based utility is negative (the coefficients  $p$  are so), a prefactor less than unity increases the utility of EVs proportionally to their rate of exposure. Since the monetary incentive applies only for EVs, we define  $u_1(t) \equiv 0$ , while  $u_2(t) \equiv u(t)$ .

By integrating (2) over time, the evolution of vehicle stock at time  $T$  is obtained as

$$S_1(T) = \eta^T S_1(t_0) + \sum_{t=t_0+1}^T \eta^{T-t} N(t) P_1(t, u(t)), \quad (10)$$

and correspondingly the total emissions at time  $T$ , obtained by integrating (3), is given as

$$\mathcal{E}(T) = \mathcal{E}(t_0) + \sum_{t=t_0+1}^T M \epsilon_1 \left( \eta^T S_1(t_0) + \sum_{t=t_0+1}^T \eta^{T-t} N(t) P_1(t, u(t)) \right), \quad (11)$$

while the total budget for the state, i.e., the sum of annual products of the incentive and the number of EV sales, is

$$I(T) = \sum_{t=t_0+1}^T u(t) N_2(t) = \sum_{t=t_0+1}^T u(t) N(t) (1 - P_1(t, u(t))). \quad (12)$$

Obviously, the higher  $u(t)$ , the less rapidly  $\mathcal{E}(T)$  increases, but at the expense of an increase in  $I(T)$ .

To find the most appropriate policy roadmap  $u(t)$ , we formulate an optimal control problem as

$$\min_{u(t)} I(T), \quad (13)$$

subject to state equations (2)-(3), the terminal condition

$$\mathcal{E}(T) \leq \overline{\mathcal{E}}, \quad (14)$$

with  $\overline{\mathcal{E}}$  as the desired emissions target at horizon  $T$ , initial condition  $\mathcal{E}(t_0) = 0$  and  $S_1(t_0)$ , and constraints on the control variable as

$$0 \leq u(t) \leq C_v^P(t). \quad (15)$$

For the discrete-time system under study, the Hamiltonian is formed as

$$\begin{aligned} H(t) = & u(t) N(t) (1 - P_1(t, u(t))) + \\ & \lambda(t) (\eta S_1(t-1) + N(t) (P_1(t, u(t)))) + \\ & \nu(t) (\mathcal{E}(t-1) + M \epsilon_1 (\eta S_1(t-1) + N(t) (P_1(t, u(t))))), \end{aligned} \quad (16)$$

so that the optimal policy roadmap, within the control bounds, is found by solving

$$\frac{\partial H(t)}{\partial u(t)} = 0. \quad (17)$$

The Euler-Lagrange equation yields the dynamics for the adjoint states  $\lambda(t)$  and  $\nu(t)$ ,

$$\begin{aligned} \lambda(t-1) &= \frac{\partial H(t)}{\partial S_1(t-1)} = \eta(\lambda(t) + M\epsilon_1\nu(t)), \\ \nu(t-1) &= \frac{\partial H}{\partial \mathcal{E}(t-1)} = \nu(t) \end{aligned} \quad (18)$$

with the initial conditions  $\lambda(t_0) = \lambda_0$ , and  $\nu(t_0) = \nu_0$ , where  $\lambda_0$  and  $\nu_0$  are to be found by imposing the terminal constraint (14) and the transversality condition  $\lambda(T) = 0$ . The solution of (18) is obtained as

$$\begin{aligned} \nu(t) &= \nu_0, \\ \lambda(t) &= \nu_0 M\epsilon_1 \eta \frac{1 - \eta^{T-t+t_0}}{1 - \eta} \end{aligned} \quad (19)$$

Assuming the constraints (15) are satisfied, we obtain the optimal solution  $u(t)$  by imposing (17), obtaining the implicit equation

$$\mathcal{Q}(t)\mathcal{R}(t)u(t)/\mathcal{P}(t) + \ln(\mathcal{R}(t))u(t) = \ln(\mathcal{R}(t))\lambda(t) + M\epsilon_1 \ln(\mathcal{R}(t))\nu(t) - 1, \quad (20)$$

where the sales  $N$  or the demand  $G$  do not appear explicitly. This transcendental equation can be solved by invoking the Lambert function<sup>1</sup>:

$$u(t) = \frac{a(t) - W(-b(t)e^{a(t)})}{c(t)}, \quad (21)$$

where  $a(t) \triangleq M\epsilon_1\nu_0 c(t) \left( \frac{\eta^{T-(t-t_0)} - \eta^{-1}}{1 - \eta^{-1}} \right) - 1$ ,  $b(t) \triangleq -\mathcal{Q}(t)/\mathcal{P}(t)$ , and  $c(t) \triangleq \ln(\mathcal{R}(t))$ .

By substituting  $u$  into (11)–(12), the target emission level and the total incentive are given by

$$\mathcal{E}(T|\nu_0) = \sum_{t=t_0+1}^T M\epsilon_1 \left( \eta^T S_1(t_0) + \sum_{t=t_0+1}^T \eta^{T-t} N(t) (1 + W(t))^{-1} \right), \quad (22)$$

$$I(T|\nu_0) = \sum_{t=t_0+1}^T N(t) \left( \frac{a(t) - W(t)}{c(t)} \right) W(t) (1 + W(t))^{-1}, \quad (23)$$

where we explicitly denoted the dependence of the solution on the unknown (by now) parameter  $\nu_0$ , and have written  $W(t)$  instead of  $W(-b(t)e^{a(t)})$  for the sake of brevity.

It is straightforward to show that

$$\begin{aligned} \frac{\partial}{\partial a} \left( \frac{1}{1+W} \right) &= -\frac{W}{(1+W)^3}, \\ \frac{\partial}{\partial a} \left( \frac{aW - W^2}{1+W} \right) &= \frac{W(1+a)}{(1+W)^3}. \end{aligned} \quad (24)$$

and that, consequently,  $\mathcal{E}(T|\nu_0)$  decreases and  $I(T|\nu_0)$  increases monotonically with  $\nu_0$ . Since  $I(T)$  is to be minimized, and the constraint (14) to be satisfied, it is clear that the optimal solution is obtained for the value of  $\nu_0$  such that the equality sign in (14) holds, i.e.,  $\mathcal{E}(T|\nu_0) = \bar{\mathcal{E}}$ . Unfortunately, it is not possible to find this value in closed form. However, it can be found numerically using a shooting algorithm.

Other sensitivities of  $\mathcal{E}(T)$ ,  $I(T)$  with respect to key parameters can be evaluated analytically. In summary the model of this section is useful to give some insight into the nature of the solutions to our backcasting problem, and to show the influence of some factors and parameters. However, it is still too simple to capture essential phenomena, so that its quantitative predictions may be inaccurate. Therefore we now move on to a more realistic model.

<sup>1</sup>The Lambert function  $W(x)$  is the solution of the equation  $We^W = x$ .

### Modeling and backcasting: Full-order model

When we reintroduce a variable mileage  $M(t)$  and  $A > 1$  age classes, the model becomes more complex, since the survival rate  $\eta_a$  and the emission factor  $\epsilon_{va}$  are now functions of age (too), and so is the old vehicle stock  $O_{va}$ .

Equation (1) is replaced by

$$E(t) = \sum_a \epsilon_{1a}(t)M(t)S_{1a}(t), \quad (25)$$

equation (2) by  $2 \times (A + 1)$  equations

$$\begin{aligned} S_{v0}(t) &= P_v(t, u(t))N(t, \mathbf{s}(t-1)) \\ S_{va}(t) &= \eta_a S_{v,a-1}(t-1), \quad \forall a = 1, \dots, A-1, \\ S_{vA}(t) &= \eta_A S_{v,A-1}(t-1) + \eta_A S_{vA}(t-1), \end{aligned} \quad (26)$$

and (3) by

$$\mathcal{E}(t) = \mathcal{E}(t-1) + \sum_a M(t)\epsilon_{1a}(t)S_{1a}(t), \quad (27)$$

where we write  $\mathbf{s} = [S_{v0}, \dots, S_{vA}]$ ,  $\forall v$ , for the stocks state vector. The explicit form of the total sales  $N(t)$  is

$$N(t, \mathbf{s}(t-1)) = \frac{G(t)}{M(t)} - \sum_{v,a=1}^{A-1} \eta_a S_{v,a-1}(t-1) + \eta_A S_{v,A-1}(t-1) + \eta_A S_{vA}(t-1), \quad (28)$$

while  $P_1(t, u(t))$  is still given by (4) and (6)–(8).

The objective function and the terminal condition for the general OCP are the same as in (13)–(14), but now the cost function is also a function of the state, due to the age dependency of the survival rates.

The Hamiltonian is formed as

$$\begin{aligned} H(t) &= u(t)(1 - P_1(u(t)))N(t, \mathbf{s}(t-1)) \\ &+ \sum_v \lambda_{v0}(t)P_v(u(t))N(t, \mathbf{s}(t-1)) \\ &+ \sum_{v,a=1}^{A-1} \lambda_{va}(t)\eta_a S_{v,a-1}(t-1) \\ &+ \sum_v \lambda_{vA}(t)\eta_A (S_{v,A-1}(t-1) + S_{vA}(t-1)) \\ &+ \nu(t) \left( \mathcal{E}(t-1) + M(t)\epsilon_{10}(t)P_1(u(t))N(t, \mathbf{s}(t-1)) \right. \\ &\quad \left. + \sum_{a=1}^{A-1} M(t)\epsilon_{1a}(t)\eta_a S_{1a-1}(t-1) \right. \\ &\quad \left. + M(t)\epsilon_{1A}(t)\eta_A (S_{1A-1}(t-1) + S_{1A}(t-1)) \right) \end{aligned} \quad (29)$$

which replaces (16), where  $\boldsymbol{\lambda} = \{\lambda_{v0}, \dots, \lambda_{vA}\}$ ,  $\forall v$  and  $\nu(t)$  are the adjoint states.

The first-order optimality conditions (17)–(18) now write

$$\frac{\partial H(t)}{\partial u(t)} = N(t, \mathbf{s}(t-1)) \left( 1 - P_1 + \frac{\partial P_1}{\partial u(t)} (M(t)\epsilon_{10}(t)\nu(t) + \lambda_{10}(t) - \lambda_{20}(t) - u(t)) \right) = 0, \quad (30)$$

$$\begin{aligned} \lambda_{va}(t-1) &= \frac{\partial H(t)}{\partial S_{va}(t-1)} = -\eta_{a+1} (u(t)(1 - P_1) + \lambda_{10}(t)P_1 + \lambda_{20}(t)(1 - P_1)) + \\ &\quad + \lambda_{v,a+1}(t)\eta_{a+1} + M(t)\nu(t)\eta_{a+1} (\delta_{v1}\epsilon_{1,a+1}(t) - P_1\epsilon_{10}(t)) \\ &\quad a = 0, \dots, A-1, \end{aligned} \quad (31)$$

$$\begin{aligned} \lambda_{vA}(t-1) &= \frac{\partial H(t)}{\partial S_{vA}(t-1)} = -\eta_A (u(t)(1 - P_1) + \lambda_{10}(t)P_1 + \lambda_{20}(t)(1 - P_1)) + \lambda_{vA}(t)\eta_A \\ &\quad + M(t)\nu(t)\eta_A (\delta_{v1}\epsilon_{1,A}(t) - P_1\epsilon_{10}(t)), \end{aligned} \quad (32)$$

Table 1: Data sources

Index	Parameter	Web link
1	$s_{voa}$	<a href="http://www.statistiques.developpement-durable.gouv.fr/parc-et-circulation">www.statistiques.developpement-durable.gouv.fr/parc-et-circulation</a>
2	$\epsilon_{1,0}$	<a href="http://carlabelling.ademe.fr/chiffrescles/r/evolutionTauxCo2">carlabelling.ademe.fr/chiffrescles/r/evolutionTauxCo2</a>
3	$e_v$	<a href="http://www.citepa.org/fr/secten">www.citepa.org/fr/secten</a>
4	$\dot{\chi}$	<a href="http://www.statistiques.developpement-durable.gouv.fr/immatriculation">www.statistiques.developpement-durable.gouv.fr/immatriculation</a>

$$\nu(t-1) = \frac{\partial H}{\partial \mathcal{E}(t-1)} = \nu(t), \quad (33)$$

where we have omitted the dependence of  $P_1$  on time and control for the sake of brevity, and  $\delta$  represents the Kronecker delta function (that is, 1 if  $v = 1$  and 0 else).

This nonlinear system of differential equations cannot be solved analytically as it was the case with (17)–(18). Therefore, numerical methods must be used. In this work we have used the trust-region constrained algorithm (*trust-constr*) within the Python *scipy.optimize* package.

### 3 RESULTS AND DISCUSSION

#### *Case study: Data*

As a case study we consider Metropolitan France to illustrate the proposed backcasting approach. For this purpose, the analysis considers a time horizon from  $t_0 = 2022$  to  $T = 2050$ , with a time step of one year. The CO<sub>2</sub> target  $\bar{\mathcal{E}}$  is set by forecasting a reference scenario in which a constant incentive (IC) of 5 k€ is provided for each EV purchased, see below.

The parameters of the model are tuned using historical data from the sources listed in Table 1. As for the survival rate, the identification was carried out using data source 1. The latter contains the historical stock of passenger cars  $s_{voa}(\tau)$  by technology, ownership type (private,  $o = 1$  and professional,  $o = 2$ ), and age until 2022. Neglecting the dependence of the survival rate on vehicle technology and the movement of second-hand vehicles between ownership types, the survival rate is evaluated as

$$\eta_a = \frac{\sum_{vo} s_{voa}(2022)}{\sum_{vo} s_{vo,a-1}(2021)}. \quad (34)$$

The initial values for the passenger car fleet is set using also data source 1 as

$$S_{va}(t_0) = s_{v1a}(2022) \text{ and } S_1(t_0) = \sum_a s_{11a}(2022). \quad (35)$$

As for the emission factor  $\epsilon_{1a}(t)$ , which considers only the apparent tailpipe emissions, the identification was carried out using two sources. Data source 2 provides the historical trend ( $\tau = 1995$  to 2020) of average CO<sub>2</sub> emissions for newly sold ( $a = 0$ ) gasoline and diesel cars. The emission factor for thermal vehicles ( $v = 1$ ) for this period is calculated as a weighted average based on the number of newly sold gasoline and diesel vehicles and their respective emission factors. For vehicles sold before 1995, the emission factor is assumed to be at the 1995 level. For the future trend ( $\tau = 2020$  to 2050), (ITF (2019)) presents the efficiency trajectory of newly sold thermal vehicles in kWh(eq.)/100 km, projecting a 50% improvement from 2015 to 2050. This trajectory, with the initial value adjusted to be consistent with data source 2, is converted to gCO<sub>2</sub>/km and approximated by a quadratic function as

$$\epsilon_{10}(\tau) = 0.01 \cdot (\tau - 2020)^2 - 1.27 \cdot (\tau - 2020) + 108.2, \quad \tau \in [2020, 2050]. \quad (36)$$

Given a stock of thermal vehicles by age, their corresponding emission factor  $\epsilon_{1a}(t)$  is obtained using the following transformation

$$\epsilon_{1a}(t) = \epsilon_{10}(t - a). \quad (37)$$

The emission factor for EVs is set to zero (i.e.,  $\epsilon_{2a} = 0$ ). The resulting values of the survival rate by vehicle age  $\eta_a$  and the emission factor of newly sold thermal vehicles  $\epsilon_{10}(\tau)$  are shown in Fig. 1.

For the annual mileage  $M(t)$ , data source 3 provides the annual CO<sub>2</sub> emissions  $e_1(\tau)$  in France. Assuming that  $M(t)$  does not depend on the vehicle type, it is evaluated as

$$M(\tau) = \frac{e_1(\tau)}{\sum_{oa} s_{1oa}(\tau)\epsilon_{10}(\tau - a)}, \quad \tau \in [2011, 2022]. \quad (38)$$

Using (38), Fig. 1 shows the annual mileage  $M(\tau)$ , with a dip during the COVID-19 pandemic in 2020. Overall,  $M(t)$  is approximated by its average of 13,500 km/y.

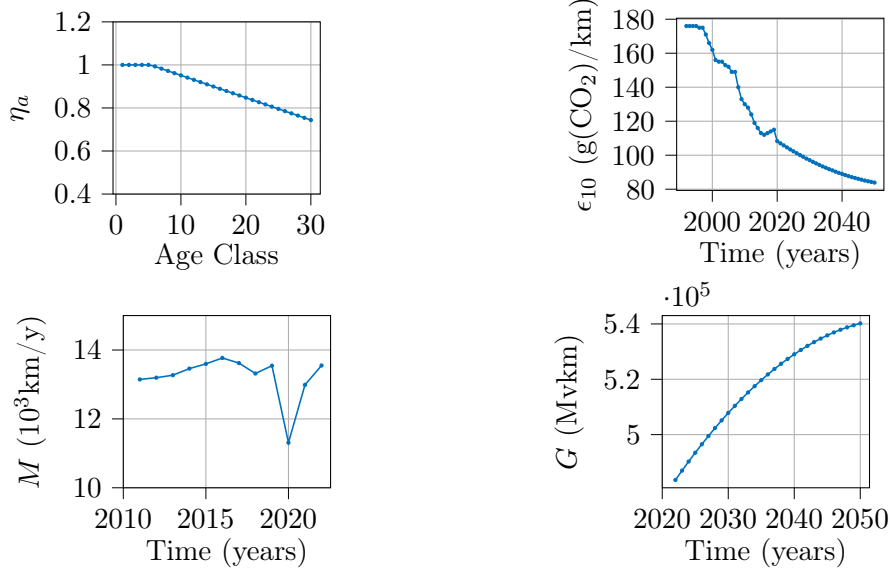


Figure 1: Model Inputs and Parameters

The parameters and determinants related to the logit model in (9) are taken from (Bouter et al. (2022)). The transport demand  $G(t)$  (vkm), shown in Fig. 1, is also taken from that work. The adoption coefficient  $c^A(t)$  is the solution of the Bass model (normalized to market share)

$$c^A(\tau) = \frac{d}{d\tau}\chi(\tau) = (p + q\chi(\tau))(1 - \chi(\tau)), \quad (39)$$

where  $p$  and  $q$  are the coefficients of innovation and imitation, respectively. The values of  $p$  and  $q$  are adjusted to match the annual EV sales from 2018 to 2022, as provided by data source 4. Figure 2 and Table 2 show the different determinants and parameters used in (9).

Table 2: List of model parameters.

Attributes	ICEV	EV
Purchase Cost ( $p^P$ )	-0.3	-0.3
Operating Cost ( $p^O$ )	-0.15	-0.15
Infrastructure Cost ( $p^I$ )	-	-0.3
$\mu$		6.75
$p$		0.02
$q$		0.4

### Reference Scenarios

In addition to the optimal and IC scenarios, we analyze three different policies, namely,

- No incentive (I0),  $u(t) \equiv 0$
- Incentive covering the entire EV price (IP),  $u(t) = C_2^P(t)$
- Ban on ICEV sales from  $t_0$  (BI),  $N_2(t) = N(t)$

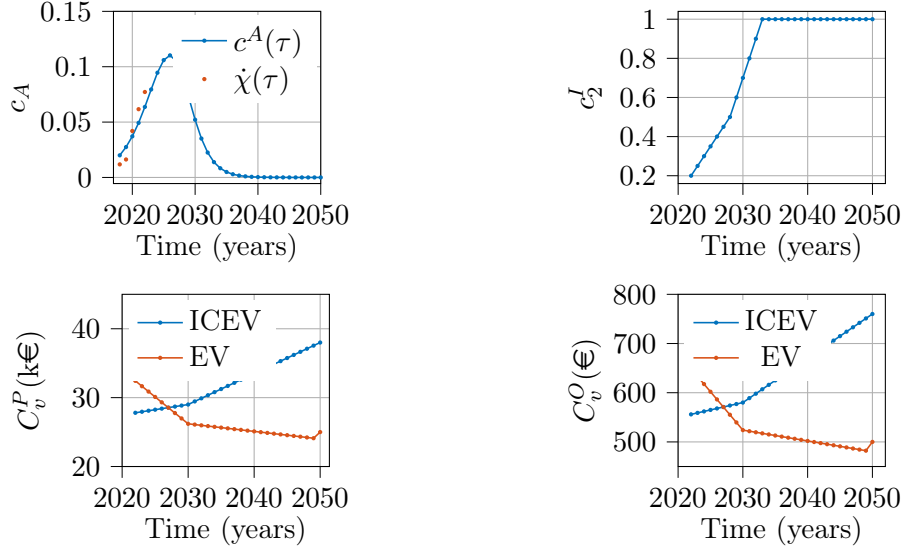


Figure 2: Determinants used in the logit model.

The corresponding curves of cumulative CO<sub>2</sub> emissions and EV stock are shown in Fig. 3. It is clear that the stricter the policy, the faster the increase in EV stock, along with a decrease in cumulative emissions. With the BI scenario, the ICEV stock is virtually depleted by 2050, and consequently the growth of cumulative CO<sub>2</sub> emissions ceases by that year. The  $\mathcal{E}(T)$  and  $I(T)$  values for the different policy scenarios are given in Table 3.

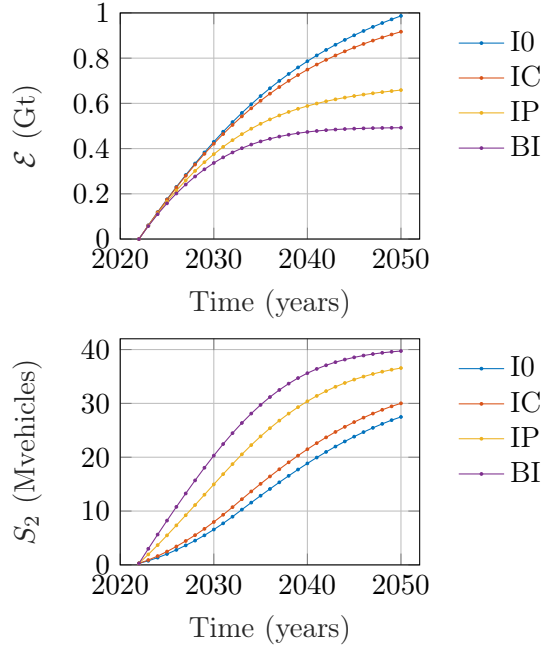


Figure 3: Reference Scenarios with the full model: CO<sub>2</sub> emissions (top) and EV stock (bottom) as a function of time.

Table 3: Reference and optimal scenario

Output	I0	IC	IP	BI	Optimal
$\mathcal{E}(T)$ (Gt)	0.98	0.91	0.65	0.49	0.91
$I(T)$ (G€)	0	215	1497	-	95.3



## Backcasting results

The IC scenario predicts a total of 0.91 Gt of CO<sub>2</sub> in 2050. Accordingly,  $\bar{\mathcal{E}}$  is first set to this value to obtain a comparable optimal incentive law.

The incentive law and emissions curves are shown in Fig. 4. The incentive law (top panel) exhibits a monotonically decreasing behavior, starting with an incentive close to 50 % of  $C_2^P(t_0)$  until being zero at a certain year. Intuitively, such behavior is optimal within the assumptions of the model, as it incentivizes early EV purchases, thereby increasing the EV share in the vehicle stock and reducing the growth of CO<sub>2</sub> emissions. This effect can be observed in the curves of EV sales and stock, as well as in the emissions curve.

The vehicle sales and stock curves for the optimal and IC scenarios are shown in Fig. 5. Compared to the IC law, EV sales are higher in the early years and begin to decrease at 2030. Clearly, in both scenarios, the ICEV stock ( $v = 1$ ) decreases while the EV stock ( $v = 2$ ) increases over time, both exhibiting an S-shaped curve suggesting a variable rate. However, towards the end, the EV stock in the optimal scenario is lower compared to the IC scenario because the optimal strategy focuses on meeting the set final emission constraint. The final cumulative CO<sub>2</sub> emissions for both scenarios are the same by construction (constraint at  $T$  imposed on the optimal scenario).

Consequently, Fig. 4, the optimal yearly emissions curve (bottom-left panel) decreases rapidly in the early years and the cumulative emissions curve (bottom-right panel) exhibits a slower growth. Overall, we obtain a total expenditure of  $I(T) = 95.3$  G€, i.e., a reduction of about 55% compared to the IC reference scenario, see Table 3.

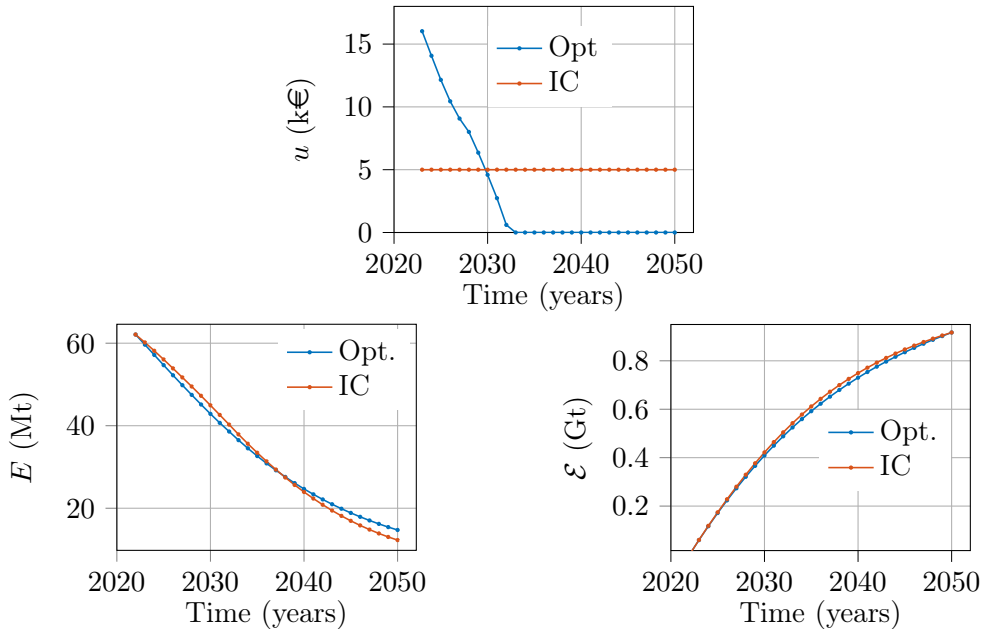


Figure 4: Incentive (top), Yearly Emission (bottom left), and Cumulative Emission (bottom right) Profile

Letting the target on  $\mathcal{E}(T)$  vary, we obtain a Pareto optimal trade-off between cumulative CO<sub>2</sub> and the total incentive, shown in Fig. 6. The rightmost point indicates the cumulative CO<sub>2</sub> emissions at  $T$  without any incentive from the state (scenario I0). Conversely, the leftmost point corresponds to the cumulative CO<sub>2</sub> emissions at  $T$ , beyond which the incentives for EVs would exceed their purchase price. It can be seen that the total incentive increases non-linearly with emissions reduction, indicating diminishing returns.

## 4 CONCLUSIONS

This study represents a first attempt to develop a backcasting methodology to identify the optimal policy roadmaps in transportation systems. The analysis focused on a passenger car fleet subsystem, describing its evolution and associated emissions, with the monetary incentive to purchase electric vehicles as the control input. The optimal incentive roadmap was derived by formulating an optimal control problem with the objective of minimizing the government budget while achiev-

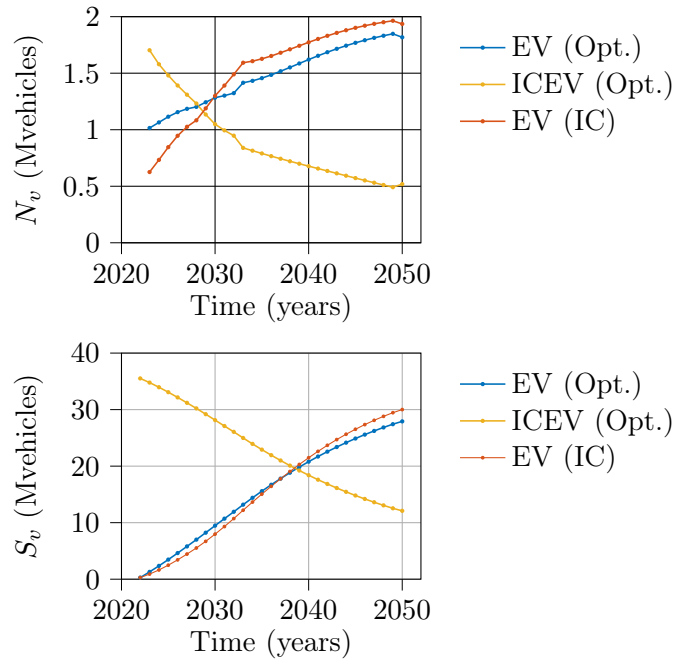


Figure 5: Vehicle Sales (top) and Vehicle Stock (bottom)

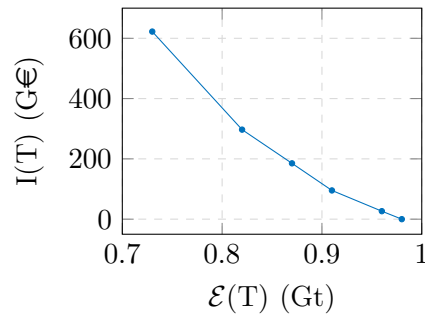


Figure 6: Pareto Optimal - Incentive vs. Cumulative Emission

ing a desired  $\text{CO}_2$  target. A quantitative case study applied to Metropolitan France was conducted to illustrate the backcasting approach.

Further research can improve the backcasting paradigm in several ways. Refinements to the fleet model could include regional disaggregation within Metropolitan France, additional vehicle types (e.g., gasoline, diesel, hybrid) and transport modes (e.g., bicycles, rail). Mileage assumptions could be refined by accounting for variation by vehicle type and user profile as in (ITF (2019)). The survival rate, currently based only on natural obsolescence, could also include factors such as Low Emission Zones (LEZ), which may accelerate vehicle turnover. In addition, the choice of LEZ implementation could be optimized. Finally, to capture the changes in operating costs and vehicle ownership, the demand for passenger cars, treated here as exogenous, could be replaced by a demand model that predicts vkm by mode and zone.

## ACKNOWLEDGEMENTS

This research benefited from state aid managed by the *Agence Nationale de la Recherche (ANR)*, under France 2030, within the project FORBAC bearing the reference ANR-23-PEMO-0002. The authors would like to acknowledge the useful discussions with Dr. Benoit Cheze (IFPEN) and the partners of the FORBAC project.

## REFERENCES

- Ashina, S., Fujino, J., Masui, T., Ehara, T., & Hibino, G. (2012). A roadmap towards a low-carbon society in japan using backcasting methodology: Feasible pathways for achieving an 80% reduction in co2 emissions by 2050. Energy Policy, 41, 584–598. doi: 10.1016/j.enpol.2011.10.053
- Bass, F. M. (1969). A new-product growth model for consumer durables. Management Science, 15(1), 215–227.
- Ben-Akiva, L., & Lerman, S. R. (2000). Discrete choice analysis. Cambridge, MA: MIT Press.
- Bibri, S. E., & Krogstie, J. (2019). A scholarly backcasting approach to a novel model for smart sustainable cities of the future: strategic problem orientation. City, Territory and Architecture, 6(3), 1–27. doi: 10.1186/s40410-019-0102-3
- Bouter, A., et al. (2022). Etude énergétique, économique et environnementale du transport routier à horizon 2040 (e4t 2040) (Tech. Rep.). IFPEN-ADEME.
- De Ceuster, G., et al. (2004). Tremove 2.2 model and baseline description (Tech. Rep.). European Commission.
- European Commission. (2021). European green deal: Commission proposes transformation of eu economy and society to meet climate ambitions (Tech. Rep.). (Press Release)
- Gomi, K., Ochi, Y., & Matsuoka, Y. (2011). A systematic quantitative backcasting on low-carbon society policy in case of kyoto city. Technological Forecasting and Social Change, 78(5), 852–871. doi: 10.1016/j.techfore.2011.01.005
- ITF. (2019). Understanding consumer vehicle choice: A new car fleet model for france (Tech. Rep.). OECD Publishing, Paris.
- Kenta, S., & Nakata, T. (2020). Recoverability analysis of critical materials from electric vehicle lithium-ion batteries through a dynamic fleet-based approach for japan. Sustainability, 12(1), 147.
- McManus, W., & Senter, R. (2009). Market models for predicting phev adoption and diffusion. (Final Report)
- Papazikou, E., et al. (2020). Detailed list of sub-use cases, applicable forecasting methodologies and necessary output variables (Tech. Rep.). Deliverable D4.4 of the H2020 project LEVITATE.
- Robinson, J. (1982). Energy backcasting—a proposed method of policy analysis. Energy Policy, 12(4), 337–344. doi: 10.1016/0301-4215(82)90048-9
- Struben, J., & Sterman, J. (2008). Transition challenges for alternative fuel vehicle and transportation systems. Environment and Planning B, 35(6), 1070–1097.
- Thorne, R., Aguilar Lopez, F., Figenbaum, E., Fridstrøm, L., & Müller, D. B. (2021). Estimating stocks and flows of electric passenger vehicle batteries in the norwegian fleet from 2011 to 2030. Journal of Industrial Ecology, 25(6), 1377–1706.
- Train, K. E. (2003). Discrete choice methods with simulation (2nd ed.). Cambridge: Cambridge University Press.
- Van Grol, R., et al. (2016). Elasticities and equations of the high-tool model (final version) (Tech. Rep.). (HIGH-TOOL Deliverable D4.3, project cofunded by the European Commission under the 7th Framework Programme, Karlsruhe)
- Woody, M., Keoleian, G. A., & Vaishnav, P. (2023). Decarbonization potential of electrifying 50% of u.s. light-duty vehicle sales by 2030. Nature Communications, 14, 7077.